Available online at www.sciencedirect.com

ScienceDirect

Procedia Computer Science 181 (2021) 931–939

Procedia Computer Science

www.elsevier.com/locate/procedia

CENTERIS - International Conference on ENTERprise Information Systems / ProjMAN - International Conference on Project MANagement / HCist - International Conference on Health and Social Care Information Systems and Technologies 2020

Atrial fibrillation classification based on MLP networks by extracting Jitter and Shimmer parameters

Pedro Henrique Borghi[a,b]*, Renata Coelho Borges[b], João Paulo Teixeira[a]

[a]*Research Centre in Digitalization and Intelligent Robotics (CEDRI), UNIAG, Instituto Politecnico de Bragança, Braganca, Portugal*
[b]*Federal University of Technology - Paraná (UTFPR), Cornélio Procópio, 86300-000, Brazil*

Abstract

Atrial fibrillation (AF) is the most common cardiac anomaly and one that potentially threatens human life. Due to its relation to a variation in cardiac rhythm during indeterminate periods, long-term observations are necessary for its diagnosis. With the increase in data volume, fatigue and the complexity of long-term features make analysis an increasingly impractical process. Most medical diagnostic aid systems based on machine learning, are designed to automatically detect, classify or predict certain behaviors. In this work, using the PhysioNet MIT-BIH Atrial Fibrillation database, a system based on MLP artificial neural network is proposed to differentiate, between AF and non-AF, segments and ECG's features, obtaining average accuracy of 80.67% in test set, for the 10-fold cross-validation method. As a highlight, the extraction of jitter and shimmer parameters from ECG windows is presented to compose the network input sets, indicating a slight improvement in the model's performance. Added to these, Shannon's and logarithmic energy entropies are determined, also indicating an improvement in performance related to the use of fewer features.

Peer-review under responsibility of the scientific committee of the CENTERIS - International Conference on ENTERprise Information Systems / ProjMAN - International Conference on Project MANagement / HCist - International Conference on Health and Social Care Information Systems and Technologies 2020

* Corresponding author. Tel.: +351 913 835 373; Tel.: +55 14 99716 6671.
E-mail address: pedromelo@alunos.utfpr.edu.br

1877-0509 © 2021 The Authors. Published by Elsevier B.V.

Peer-review under responsibility of the scientific committee of the CENTERIS - International Conference on ENTERprise Information Systems / ProjMAN - International Conference on Project MANagement / HCist - International Conference on Health and Social Care Information Systems and Technologies 2020
10.1016/j.procs.2021.01.249

Keywords: Atrial Fibrillation; Logarithm Energy; Shannon Entropy; Jitter of ECG; Shimmer of ECG.

1. Introduction

Atrial fibrillation (AF) is the most common cardiac anomaly and one that potentially threatens human life. It is a cardiac anomaly represented strongly by a non-uniform and prolonged variation in heart rate. This variation can happen in very short periods to days [1]. Morphologically it is related not only to the loss of atrial contraction (attenuation of the P wave) but also to the rapid and irregular contraction of the ventricles [2]. It is estimated that approximately 1% of the world population has its anomaly, making it the most common and sustainable among cardiac disorders [3].

It is expected that the increase on the rate of AF occurs by increasing age of the patient, especially after age 60 [3]. Although many cases are asymptomatic, the subjects may present symptoms such as tiredness, indisposition and chest pain. In addition to decreasing life quality, as it persists, it can lead to the development of ventricular dysfunction, coronary artery disease, stroke, among others, leading to imminent fatal risks [2].

Long-term monitoring of cardiac activity is known to increase the likelihood of diagnosing paroxysmal atrial fibrillation [1], being this topology defined by episodes that end spontaneously without pharmacological or electrical intervention within up to seven days [2]. If intervention is required, the typology is defined as persistent and, if it could not be stopped by interventions and remaining for periods of more than one year, it is defined as permanent [2].

The most common way to obtain and analyze a patient's cardiac activity is through an electrocardiogram (ECG). Despite an effort by health professionals to tighten the standards for diagnosis, the difficulties become even more expressive when the duration of ECG signals is in the order of several hours, associating the chances of human error with tiredness and the intrinsic tendencies to the signs, particular to each patient [1]. Thus, the relevance of an automatic and accurate computer system for the interpretation of ECG signals and aid in medical diagnosis becomes evident. Such systems reduce the fatigue factor and the susceptibility to the human error, operating only limited by the structural capabilities of hardware and inevitable approaches in the digital domain [4].

The manual feature extraction depends mainly on the experience and prior knowledge of specialists and doctors [5]. The composition and extraction of sets of characteristics is found in various forms in the literature, for example, morphological features [6-7], temporal features [6, 8], hermite basis function (HBF) [9], higher order statistics (HOS) [10], Discrete Cosine Transform (DCT) [11], Discrete Fourier Transform (DFT) [12-13] personalized features [14], auto-encoders [15], Wavelet transform [6, 16], Common Spatial Pattern (CSP) [17], entropies [18], Variational Mode Decomposition (VDM) [19], auto regressive models [20], Stacked Sparse Autoencoders (SSAE) [21] and convolutional blocks [22].

Regarding the learning and classification models, it is possible to separate them into two major approaches with several specific algorithms. The first, traditional machine learning, has as examples: k-nearest neighbor [10], support vector machine (SVM) [6], Multi-Layer Perceptron (MLP) [23], conditional random fields [24], evolutionary neural system [12], random forest (RF) [19] e Linear Discriminant Analysis (LDA) [25]. The second, based on deep learning, replaces in most applications, the need for manual extraction of resources, abstracting the expression and generalization of nonlinear characteristics of the input into a single structure [26]. The usual structures of this approach are: convolutional neural networks (CNN) [27], traditional recurrent neural networks (RNN) [28], LSTM (Long Short-Term Memory) [27], Gated Recurrent Unit (GRU) [26] and Convolutional Autoencoder (CAE) [29].

Faust et al. [1] developed a system for assisting medical diagnosis based on a bilateral LSTM network (BLSTM) for the detection of atrial fibrillation in windows with 100 heartbeats. The data were acquired from the PhysioNet MIT-BIH Atrial Fibrillation platform. Apart from segmentation, no other pre-processing function has been implemented. The accuracy obtained on the test set after applying the 10-fold cross-validation strategy was 98.51%.

H. Dang et al. [27] proposed the combination of CNN and BLSTM for automatic analysis of ECG signals in order to detect occurrences of atrial fibrillation. For that, it used the PhysioNet data set MIT-BIH Atrial Fibrillation, and the recordings went through stages of event detection, segmentation and Z-score normalization. With the exception of creating the arrangement of the input sets, there was no manual extraction of characteristics. The accuracy obtained for the proposed model was 96.59%.

This work proposes the use of the MLP machine learning model [30], exploring its performance for several general parameter arrangements, methodologically presented in Section 4.

Although systems based on deep learning networks (namely CNN and LSTM) are superior in accuracy to other models, they are extremely costly in computational complexity and require much more extensive data sets to be trained [30]. On the other hand, the MLP architecture can achieve sustainable results of accuracy even with exchange for a reduction in computational cost, allowing the exploitation of many arrangements in less time.

As an innovative factor of this work, the investigation of the extraction and association of jitter and shimmer parameters of ECG signals to the data set used as input for MLP models is presented. This work also aims to introduce the investigation and development of a practical computational system to aid medical diagnosis with functionality not only for interpreting and classifying input data, but also for forecasting events, placing most of the approaches found in focus in the literature, where the majority opts for the classification.

2. Theoretical Framework

2.1. Jitter

Since the occurrence of AF is strongly related to a frequent variation in cardiac rhythm, the extraction of ECG parameters that represent this behavior in a more descriptive way than the ECG itself, becomes potentially attractive due to possible collaboration in the learning process of artificial neural networks.

According to [26-27], four jitter parameters can be determined in a time window. These parameters separately indicate: the mean absolute difference between consecutive periods (*J1*); the mean absolute difference between consecutive periods divided by the mean window period (*J2*); the relative average disturbance given by the mean absolute difference between each period and the mean of this and two adjacent divided by the average window period (*J3*); and the five-point period disturbance quotient given by the average absolute difference between each period and the average of this and its four neighbors divided by the average window period (*J4*). The equations (1) to (4) express, respectively, the presented jitter parameters, where N is the window size, T_i is the current period and T_n is the period relative to T_i in calculating the mean.

$$J1 = \frac{1}{N-1}\sum_{i=1}^{N-1}|T_{i+1} - T_i| \ [s] \tag{1}$$

$$J2 = \frac{\frac{1}{N-1}\sum_{i=1}^{N-1}|T_{i+1} - T_i|}{\frac{1}{N}\sum_{i=1}^{N} T_i} * 100 \ [\%] \tag{2}$$

$$J3 = \frac{\frac{1}{N-1}\sum_{i=2}^{N-1}\left|T_i - \left(\frac{1}{3}\sum_{n=i-1}^{i+1} T_n\right)\right|}{\frac{1}{N}\sum_{i=1}^{N} T_i} * 100 \ [\%] \tag{3}$$

$$J4 = \frac{\frac{1}{N-1}\sum_{i=3}^{N-2}\left|T_i - \left(\frac{1}{5}\sum_{n=i-2}^{i+2} T_n\right)\right|}{\frac{1}{N}\sum_{i=1}^{N} T_i} * 100 \ [\%] \tag{4}$$

2.2. Shimmer

Since AF events distort the heartbeat morphology, it is relevant to extract characteristics related to their amplitude. The shimmer appears as an option to perform this function since it describes the variation in amplitude of consecutive periods within a window [31]. Four shimmer parameters can be calculated: absolute average of the logarithm of the rate between amplitudes of two adjacent periods (*S1*); average absolute difference between amplitudes of two adjacent periods divided by the mean amplitude of the window (*S2*); three-point amplitude disturbance quotient the average absolute difference between the amplitude of each period and the mean between this and that of two adjacent ones divided by the mean amplitude of the window (*S3*); and the five-point amplitude disturbance quotient being the average absolute difference between the amplitude of each period and the average between this and that of four neighbors divided by the mean amplitude of the window (*S4*). Respectively to S1 to S4, equations (5) to (8) present their relations, where A_i is the amplitude of the current period and A_n is the period relative to the current period in the calculation of the average.

$$S1 = \frac{1}{N-1}\sum_{i=1}^{N-1}\left|20 * \log\left(\frac{A_{i+1}}{A_i}\right)\right| \; [dB] \tag{5}$$

$$S2 = \frac{\frac{1}{N-1}\sum_{i=1}^{N-1}|A_i - A_{i+1}|}{\frac{1}{N}\sum_{i=1}^{N} A_i} * 100 \; [\%] \tag{6}$$

$$S3 = \frac{\frac{1}{N-1}\sum_{i=2}^{N-1}\left|A_i - \left(\frac{1}{3}\sum_{n=i-1}^{i+1} A_n\right)\right|}{\frac{1}{N}\sum_{i=1}^{N} A_i} * 100 \; [\%] \tag{7}$$

$$S4 = \frac{\frac{1}{N-1}\sum_{i=3}^{N-2}\left|A_i - \left(\frac{1}{5}\sum_{n=i-2}^{i+2} A_n\right)\right|}{\frac{1}{N}\sum_{i=1}^{N} A_i} * 100 \; [\%] \tag{8}$$

2.3. Shannon Entropy and Logarithm Energy

Another way of extracting information regarding not only the beat's morphology but also their duration, within a set of beats, is through the calculation of entropies. For certain types of entropies, longer signal windows generally result in better descriptions of atrial fibrillation events when compared to short periods, as they provide greater contextualization [18].

Among the several entropies found in the literature, two of them are selected to compose the system, Shannon (E_{sh}) and energy logarithm (E_{logen}). The first provides a measure of the probabilistic distribution of the segment information. The second provides an estimate of the complexity intensity of the segment. Both entropies are expressed respectively by equations (9) and (10), where E_n are the samples of signal energy.

$$E_{sh} = -\sum_{n=1}^{N} (\mathrm{E_n} * \log_2(E_n)) \tag{9}$$

$$E_{logen} = \sum_{n=1}^{N} \log(E_n^2) \tag{10}$$

2.4. Normalization

Normalization of input data is essential for machine learning models based on artificial neural networks, in order to minimize problems such as data redundancy and distorted results for inputs representing anomalies [32]. The standardization method used in this work on the extracted characteristics was the standardized z-score normalization [33]. Equation (11) represents the generic form of calculating the z-score normalization for a sequence of samples x, where $\bar{X}$ is its mean, S the standard deviation and z the normalized output. Moreover, Figure 1 show an example of applying z-score normalization and standard normalization with [-1,1] range on a non-normalized data vector.

$$z = \frac{x - \bar{X}}{S} \tag{11}$$

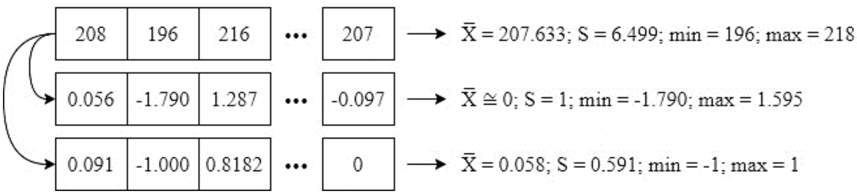

Fig. 1. Example of data normalization over a sequence of consecutive R-peak intervals at a random ECG record. First vector represents the non-normalized data. The second vector represents the data after z-score function been applied over the first. The third vector represents the data after standard [-1,1] normalization been applied over the first.

3. Materials

The database used was extracted from MIT-BIH Atrial Fibrillation [34-35], available public and freely through the PhysioNet digital platform [36]. On this basis, there are 25 long-term ECG recordings (10 hours in duration), among which 23 are represented both by the electrode signals in two leads, the rhythmic annotations performed by medical specialists and detection of R peaks. Another two recordings are made available only by the notes and, therefore, are discarded by this experiment. ECG signals are digitalized at a sampling frequency of 250 Hz with a 12-bit resolution over a range of ± 10 mV.

To conduct the experiments, a computer with an Intel® Core™ i7-6500U 2.5GHz processor, 8GB of RAM and a GeForce 920MX 2GB video card was used. The proposed system algorithm was implemented and executed in MatLab® 2020a software, using the Deep Learning Toolbox.

4. Methodology

Initially, the data present in the MIT-BIH Atrial Fibrillation database were downloaded, differentiating the recordings between patients. The data were organized in such a way that each patient had recordings of two leads from the ECG itself and the respective references of rhythms and detection of the R peaks. Thus, for this work, the marks already present in the database were used. Signal acquisition was performed with the help of the WFDB Toolbox for Matlab® [37-38]. No steps of filtering or removing trends from the signals were implemented, being used in its raw form.

Then, the recordings were segmented taking into account the difference in samples between adjacent R peaks. For this, the indexes of the R peak marks of the signals were used. From this information, segments of 30 consecutive intervals (RRi) were constructed with a 10 RRi sliding between adjacent segments. In this way, it is possible to increase the number of examples to the learning system, reducing the effect of short dataset. Following, still using the locations of the R peaks, their amplitudes, for the two leads, were stored for later calculation of the Shimmer parameters.

The process of assigning a new reference for the 30 RRi segments generated was then made. In this, a factor of proportion μ was considered empirically as a threshold between the two classes. Comparing the indexes of each RRi with the rhythmic reference of the database, a segment of 30 RRi was assigned the reference of atrial fibrillation if at least μ (percentage) of intervals belonged to an atrial fibrillation event. Otherwise, the interval was considered not to be atrial fibrillation, regardless of the signal behavior. The two categories were organized in a binary way in two lines, so that the learning system had two outputs and thus directed each one to specialize a category. To assess the balance of the generated data set, the ratio between the number of segments named atrial fibrillation and the total was determined.

In the process of feature extraction, to be associated with the 30 RRi segments, the jitter, shimmer and Shannon and logarithm energy entropies parameters were determined. The data normalization step was implemented using the standard z-score function. For each feature of the segment, the function was applied separately, the 30 RRi being considered a single feature. That is, for each segment, the 30 RRi resulted in approximately average 0 and standard deviation 1, while separately for each pattern of jitter, shimmer and entropies, this approximation occurred between all segments of each subject.

In preparation for the training and testing of the neural network, the data set was divided according to the number of selected subjects, this allows the network to be evaluated in the test according to its ability to generalize not only data not seen in training but also to ECG of new patients. Two methodologies for organizing the sets were carried out. The first methodology, used in a preliminary step in the process of choosing network parameters (number of hidden layers, number of neurons and activation functions), was based, in each iteration, on a random choice of 5 subjects for testing, 3 subjects for validation during training and 15 subjects for training. The second methodology, used in the final model, consisted of using the 10-fold cross validation method. This method consists of generating ten different combinations of subjects for training and testing, with each subject belonging to a single set per combination. The validation set during the training of the network was defined randomly from all samples of the training set, being only parameterized by the proportion of 15% of the training set.

The process of choosing the neural network architecture and parameters was made with the first methodology, according to the following steps:

- Selection of the data set whose μ = 30%;
- Generation of input sets according to the first methodology;
- Repetition of training and testing for the same model five times, in order to reduce the effect of assigning random initial synaptic weights and possible early training stops;
- Variation of the activation functions of the hidden and output layers: tangent sigmoid and logistic sigmoid;
- Variation of the number of neurons in each hidden layer between 40 and 195 neurons;
- Variation of the number of hidden layers from 1 to 4;
- Set the training algorithm as Resilient Backpropagation.

The evaluation of each model was based on the average accuracy produced after selecting several sets of random segments. From the observation of the results, the models whose accuracy results were greater than 85% were selected. Two models were selected. Then the models were evaluated, by measuring training and test accuracy, for the three data sets (μ = [10%; 30%; 50%]) according to the generation of input sets of the second methodology.

However, for practical observation of the relevance of the input features, the process were carried out for different combinations of features in the input sets, using the two selected models. Four compositions were developed, as it follows, where the indices in the shimmer parameters and in both entropies indicate the lead of the ECG from which they were calculated:

- Comp_01: 30 RRi (length of RR interval);
- Comp_02: Comp_01 + $J1 + J2 + J3 + J4$;
- Comp_03: Comp_02 + $S1_1 + S1_2 + S2_1 + S2_2 + S3_1 + S3_2 + S4_1 + S4_2$;
- Comp_04: Comp_03 + $E_{sh1} + E_{sh2} + E_{logen1} + E_{logen2}$.

5. Results

After performing the segmentation process and re-referencing the ECG recordings, the proportions obtained from segments named atrial fibrillation relative to the total of segments ($K = 112\ 797$) for three values of μ, 10%, 30% and 50%, are respectively , 55%, 53% and 45%. There is a certain balance in the proportion of the categories since they are approximately 5% away from the central value. With this datasets distribution the unbalanced problems were avoided.

The process of choosing the most efficient parameters for the MLP network, within the specifications predetermined in the first methodology and evaluated for accuracy, resulted in two architectures (ML_01 and ML_02), shown in Table 1. In this, it is possible to notice the exclusivity of the tangent sigmoid activation function, in the hidden layers.

Table 1. Results of the preliminary step (first methodology) of choosing parameters for the MLP network.

	Number of Hidden Layers	Neurons by Hidden Layer	Activation Function	Average Accuracy in Test Set [%]
ML_01	3	165	Tan-sig	85,45
ML_02	3	180	Tan-sig	86,29

Table 2. Accuracy for 10-fold cross validation in the test set (all dataset, with 112797 segments) for both models.

	Comp_01			Comp_02			Comp_03			Comp_04		
μ [%]	10	30	50	10	30	50	10	30	50	10	30	50
ML_01	76.66	73.66	76.70	80.00	72.56	77.50	79.52	74.94	78.73	**80.67**	75.47	80.47
ML_02	78.31	73.16	75.75	76.10	70.33	77.96	77.05	71.95	73.87	80.33	72.08	**80.61**

Table 2 shows the sequence of experiments for the second methodology, with the three datasets and different arrangements of input features, on the two architectures. There is a slight improvement in the performance of the models as more input data are provided, except for the shimmer parameter. Its relevance can be considered weak due to the reference used for its calculation (amplitude of the R peaks). Although AF is related to disturbances in the depolarization of the ventricles (R wave), its amplitude is not relevant to the models.

Also according to Table 2, the ML_01 learning model presents slightly higher results than the ML_02, with the best performance (80.67% accuracy) observed in the use of all features and in the 10% choice for the μ factor. It is notable that the factor μ = 30% provides inferior results to the others, with the factor μ = 10% reaching the best performance. Considering the results for parameter μ = 10%, it can be said that the presence of little information about AF, in a small proportion a 30-beat window is sufficient to identify the anomaly of that specific characteristics.

6. Conclusions

In this work, atrial fibrillation recognition experiments based on segmentation and extraction of ECG signal features on intervals of 30 consecutive R peaks were presented. The learning model, MLP artificial neural network, was submitted to some input sets composed of four combinations of features and demonstrated a slight increase in accuracy as more features were introduced. The best result (80.67% accuracy in the test set) was achieved by the architecture with 3 hidden layers, 165 neurons in each layer, tangent sigmoid activation function, use of all the features in the input set and considering an AF segments when 10% of RR intervals are labeled as AF.

The extraction of the jitter and shimmer parameters of the signals is highlighted as an innovative element and it is proposed to continue the investigation of its applications on different regions of the heartbeat, in the case of the shimmer, and on different sizes of segments.

For future works, the feature set may be expanded on different entropy methods, analysis in the frequency domain and statistical measures. For the learning and classification model, the feedback element between the layers can be included to investigate the memory effect on the models already obtained, performing new experiments based on the jitter and shimmer parameters on, for example, LSTM deep learning networks.

Acknowledgements

This work has been supported by FCT – Fundação para a Ciência e Tecnologia within the Project Scope: UIDB/05757/2020.

References

[1] O. Faust, A. Shenfield, M. Kareem, T. R. San, H. Fujita, and U. R. Acharya. (2008) "Automated detection of atrial fibrillation using long short-term memory network with RR interval signals," *Comput. Biol. Med.*, vol. 102, no. July, pp. 327–335, 2018, doi: 10.1016/j.compbiomed.2018.07.001.

[2] V. Markides and R. J. Schilling. (2003) "Atrial fibrillation: Classification, pathophysiology, mechanism and drug treatment," *Heart*, vol. 89, no. 8, pp. 939–943, doi: 10.1136/heart.89.8.939.

[3] S. Petrutiu, J. Ng, G. M. Nijm, H. Al-Angari, S. Swiryn, and A. V. Sahakian. (2006) "Atrial fibrillation and waveform characterization: A time domain perspective in the surface ECG," *IEEE Engineering in Medicine and Biology Magazine*, vol. 25, no. 6. Institute of Electrical and Electronics Engineers Inc., pp. 24–30, doi: 10.1109/EMB-M.2006.250505.

[4] J. P. Teixeira and A. Ferreira. (2015) "Ambulatory Electrocardiogram Prototype," in *Procedia Computer Science*, vol. 64, pp. 800–807, doi: 10.1016/j.procs.2015.08.631.

[5] R. Li, X. Zhang, H. Dai, B. Zhou, and Z. Wang. (2019) "Interpretability Analysis of Heartbeat Classification Based on Heartbeat Activity's Global Sequence Features and BiLSTM-Attention Neural Network," *IEEE Access*, vol. 7, pp. 109870–109883, doi: 10.1109/access.2019.2933473.

[6] Ö. Yıldırım, P. Pławiak, R. S. Tan, and U. R. Acharya. (2018) "Arrhythmia detection using deep convolutional neural network with long duration ECG signals," *Comput. Biol. Med.*, vol. 102, no. August, pp. 411–420, doi: 10.1016/j.compbiomed.2018.09.009.

[7] J. P. Teixeira, and V. Lopes. (2011) "Electrocardiogram events detection," in *Communications in Computer and Information Science*, vol. 221 CCIS, no. PART 3, pp. 307–316, doi: 10.1007/978-3-642-24352-3_33.

[8] Teixeira, J. P. and Freitas D. (2003). "Segmental Durations Predicted With a Neural Network", Proceedings of Eurospeech'03 – International Conference on Spoken Language Processing, Geneva. Pages 169-172.

[9] K. S. Park *et al.*. (2008) "Hierarchical support vector machine based heartbeat classification using higher order statistics and hermite basis function," in *Computers in Cardiology*, vol. 35, pp. 229–232, doi: 10.1109/CIC.2008.4749019.

[10] Y. Kutlu and D. Kuntalp. (2012) "Feature extraction for ECG heartbeats using higher order statistics of WPD coefficients," *Comput. Methods Programs Biomed.*, vol. 105, no. 3, pp. 257–267, doi: 10.1016/j.cmpb.2011.10.002.

[11] R. J. Martis, U. R. Acharya, C. M. Lim, and J. S. Suri. (2013) "Characterization of ECG beats from cardiac arrhythmia using discrete cosine transform in PCA framework," *Knowledge-Based Syst.*, vol. 45, pp. 76–82, doi: 10.1016/j.knosys.2013.02.007.

[12] P. Pławiak. (2018) "Novel methodology of cardiac health recognition based on ECG signals and evolutionary-neural system," *Expert Syst. Appl.*, vol. 92, pp. 334–349, doi: 10.1016/j.eswa.2017.09.022.

[13] Rodrigues, P. M.; Teixeira, João Paulo. (2010) "Classification of Electroencephalogram Signals Using Artificial Neural Networks". Proceedings of 3rd International Conference on BioMedical Engineering and Informatics (BMEI'10)

[14] P. Cheng and X. Dong. (2017) "Life-threatening ventricular arrhythmia detection with personalized features," *IEEE Access*, vol. 5, pp. 14195–14203, doi: 10.1109/ACCESS.2017.2723258.

[15] M. M. A. Rahhal, Y. Bazi, H. Alhichri, N. Alajlan, F. Melgani, and R. R. Yager. (2016) "Deep learning approach for active classification of electrocardiogram signals," *Inf. Sci. (Ny).*, vol. 345, pp. 340–354, doi: 10.1016/j.ins.2016.01.082.

[16] Rodrigues, Pedro M. and Teixeira, João Paulo, (2013). "Alzheimer's Disease Recognition with Artificial Neural Networks" - chapter 7 (pag. 102-119) of the book "Information Systems and Technologies for Enhancing Health and Social Care", by Ricardo Martinho, Rui Rijo, Maria Manuela Cunha and João Varajão. IGI Global. DOI: 10.4018/978-1-4666-3667-5.

[17] S. L. Oh *et al.*. (2017) "Automated identification of coronary artery disease from short-term 12 lead electrocardiogram signals by using wavelet packet decomposition and common spatial pattern techniques," in *Journal of Mechanics in Medicine and Biology*, vol. 17, no. 7, doi: 10.1142/S0219519417400073.

[18] U. R. Acharya *et al.*. (2018) "Entropies for automated detection of coronary artery disease using ECG signals: A review," *Biocybernetics and Biomedical Engineering*, vol. 38, no. 2. PWN-Polish Scientific Publishers, pp. 373–384, doi: 10.1016/j.bbe.2018.03.001.

[19] R. K. Tripathy, L. N. Sharma, and S. Dandapat. (2016) "Detection of Shockable Ventricular Arrhythmia using Variational Mode Decomposition," *J. Med. Syst.*, vol. 40, no. 4, pp. 1–13, doi: 10.1007/s10916-016-0441-5.

[20] E. Alickovic and A. Subasi. (2015) "Effect of Multiscale PCA De-noising in ECG Beat Classification for Diagnosis of Cardiovascular Diseases," *Circuits, Syst. Signal Process.*, vol. 34, no. 2, pp. 513–533, doi: 10.1007/s00034-014-9864-8.

[21] J. Yang, Y. Bai, F. Lin, M. Liu, Z. Hou, and X. Liu. (2018) "A novel electrocardiogram arrhythmia classification method based on stacked sparse auto-encoders and softmax regression," *Int. J. Mach. Learn. Cybern.*, vol. 9, no. 10, pp. 1733–1740, doi: 10.1007/s13042-017-0677-5.

[22] M. Zihlmann, D. Perekrestenko, and M. Tschannen. (2017) "Convolutional recurrent neural networks for electrocardiogram classification," in *Computing in Cardiology*, vol. 44, pp. 1–4, doi: 10.22489/CinC.2017.070-060.

[23] M. Thomas, M. K. Das, and S. Ari. (2015) "Automatic ECG arrhythmia classification using dual tree complex wavelet based features," *AEU - Int. J. Electron. Commun.*, vol. 69, no. 4, pp. 715–721, doi: 10.1016/j.aeue.2014.12.013.

[24] G. De Lannoy, D. François, J. Delbeke, and M. Verleysen. (2012) "Weighted conditional random fields for supervised interpatient heartbeat classification," *IEEE Trans. Biomed. Eng.*, vol. 59, no. 1, pp. 241–247, doi: 10.1109/TBME.2011.2171037.

[25] Y. C. Yeh, W. J. Wang, and C. W. Chiou. (2009) "Cardiac arrhythmia diagnosis method using linear discriminant analysis on ECG signals," *Meas. J. Int. Meas. Confed.*, vol. 42, no. 5, pp. 778–789, doi: 10.1016/j.measurement.2009.01.004.

[26] H. M. Lynn, S. B. Pan, and P. Kim. (2019) "A Deep Bidirectional GRU Network Model for Biometric Electrocardiogram Classification Based on Recurrent Neural Networks," *IEEE Access*, vol. 7, pp. 145395–145405, doi: 10.1109/ACCESS.2019.2939947.

[27] H. Dang, M. Sun, G. Zhang, X. Qi, X. Zhou, and Q. Chang. (2019) "A Novel Deep Arrhythmia-Diagnosis Network for Atrial Fibrillation Classification Using Electrocardiogram Signals," *IEEE Access*, vol. 7, pp. 75577–75590, doi: 10.1109/ACCESS.2019.2918792.

[28] R. S. Andersen, A. Peimankar, and S. Puthusserypady. (2019) "A deep learning approach for real-time detection of atrial fibrillation," *Expert Syst. Appl.*, vol. 115, pp. 465–473, doi: 10.1016/j.eswa.2018.08.011.
[29] S. L. Oh, E. Y. K. Ng, R. S. Tan, and U. R. Acharya. (2019) "Automated beat-wise arrhythmia diagnosis using modified U-net on extended electrocardiographic recordings with heterogeneous arrhythmia types," *Comput. Biol. Med.*, vol. 105, pp. 92–101, doi: 10.1016/j.compbiomed.2018.12.012.
[30] S. Haykin. (2007) *Redes neurais: princípios e prática*. Bookman Editora.
[31] J. P. Teixeira and A. Gonçalves. (2016) "Algorithm for Jitter and Shimmer Measurement in Pathologic Voices," in *Procedia Computer Science*, vol. 100, pp. 271–279, doi: 10.1016/j.procs.2016.09.155.
[32] Silva, Letícia; Hermsdorf, Juliana; Guedes, Victor; Teixeira, Felipe; Fernandes, Joana; Bispo, Bruno & Teixeira, João Paulo. (2019) "Outliers Treatment to Improve the Recognition of Voice Pathologies," *Procedia Comput. Sci.*, vol. 164, pp. 678–685, doi: 10.1016/j.procs.2019.12.235.
[33] "Standardized z-scores - MATLAB zscore." [Online]. Available: https://www.mathworks.com/help/stats/zscore.html. [Acc.: 29-Apr-2020].
[34] G. B. Moody and R. G. Mark. (1992) "MIT-BIH Atrial Fibrillation Database." physionet.org, doi: 10.13026/C2MW2D.
[35] S. H. Goldberger AL, Amaral LAN, Glass L, Hausdorff JM, Ivanov PCh, Mark RG, Mietus JE, Moody GB, and Peng C-K. (2003) "PhysioBank, PhysioToolkit, and PhysioNet: Components of a New Research Resource for Complex Physiologic Signals." p. 5.
[36] "MIT-BIH Atrial Fibrillation Database v1.0.0." [Online]. Available: https://physionet.org/content/afdb/1.0.0/. [Accessed: 29-Apr-2020].
[37] I. Silva, and G. B. Moody. (2014) "An Open-source Toolbox for Analysing and Processing PhysioNet Databases in MATLAB and Octave," *J. Open Res. Softw.*, vol. 2, doi: 10.5334/jors.bi.
[38] A. L. Goldberger *et al.*. (2000) "PhysioBank, PhysioToolkit, and PhysioNet: components of a new research resource for complex physiologic signals.," *Circulation*, vol. 101, no. 23, doi: 10.1161/01.cir.101.23.e215.